

Franck-Hertz Experiment

Nestor Viana
Florida International University

November 25th, 2019

1 Introduction

First performed in 1914, the Franck-Hertz experiment marked a historical achievement in how we understand the quantum world. It proved the existence of discrete energy levels of atoms involving the electron transitions from one state to another, previously hypothesized by Bohr in his 1913 paper describing the quantization of electrons' orbital angular momentum and Maxwell's classical radiation theory regarding orbital frequency¹. Due to the remarkable importance of this discovery, German physicists James Franck and Gustav Hertz were awarded the Nobel Prize in Physics in 1925. In this experiment we replicate part of the original one to demonstrate how low-energy electron bombardment results in the excitation of Hg vapor atoms and to describe the nature of the excitation.

2 Setup

The core part of the experiment is performed in a vacuum tube containing a small amount of liquid mercury, known as a Franck-Hertz tube, located inside a heating chamber. We regulate the tube environment using a digital temperature controller and a control unit.

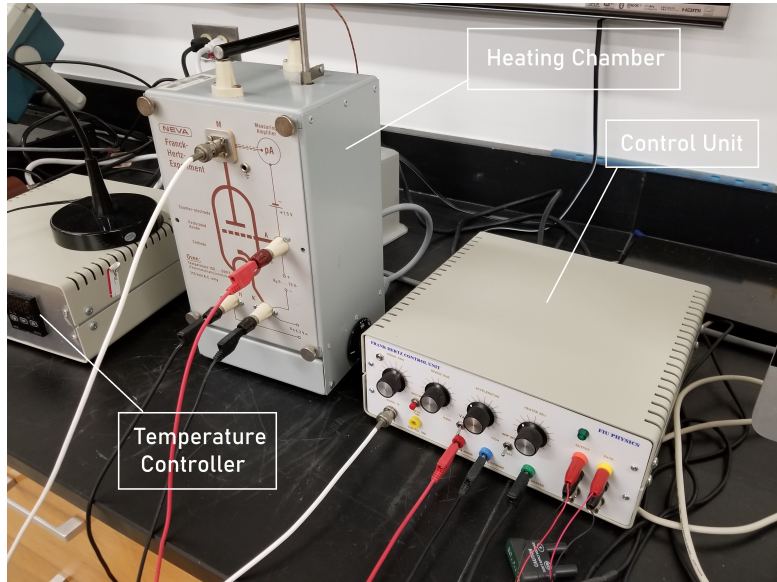


Figure 1: Experimental equipment. The Franck-Hertz tube is located inside the heating chamber.

Some of the mercury vaporizes when the temperature in the heating chamber is increased. Once electrons gain enough energy higher than the work function of the filament (cathode), the filament releases them through thermionic emission (Figure 2). In the presence of an electric field of voltage V_{acc} , the electrons accelerate through the Franck-Hertz tube and collide with the mercury atoms until they reach the accelerating grid (anode) where they encounter a retarding voltage V_d of about 1.5 V to the detector electrode.

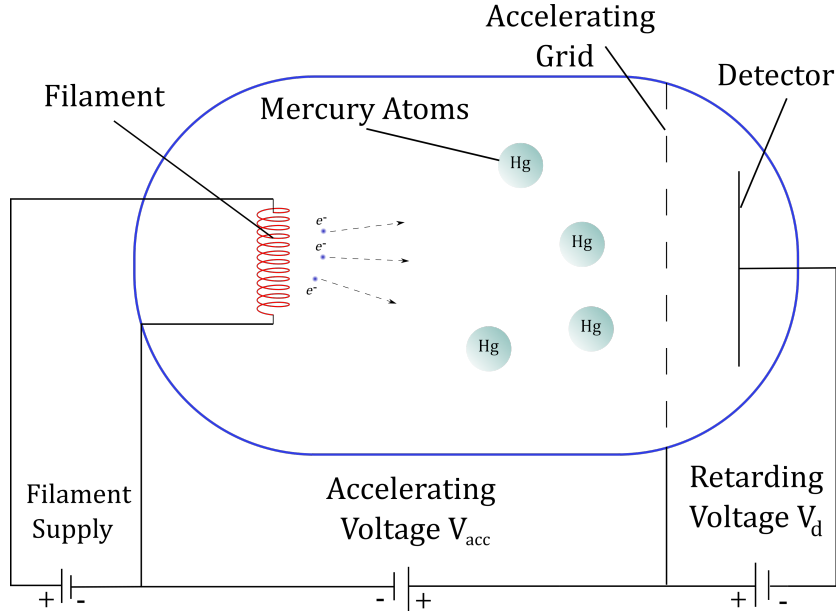


Figure 2: Franck-Hertz tube.

The nature of the collisions virtually depends on the magnitude of V_{acc} and the temperature of the heating chamber. At a higher temperature more of the liquid Hg vaporizes, increasing its *vapor pressure* and the frequency of electron-Hg collisions while shortening the *mean free path* of the electrons. Vapor pressure is the pressure a gas exerts on the surface of its liquid or solid phase in dynamic equilibrium; i.e. when the rate at which molecules enter the gas state equals the rate at which the molecules enter the liquid or solid phase. Mean free path is the average distance a molecule travels between successive collisions. Such collisions first take place inelastically without significant transfer of energy to the mercury atoms.

In Figure 3 we represent such events as electrons (a) and (b), where the kinetic energy of electrons isn't dramatically reduced after colliding and the electrons are able to reach the detector. However, when the accelerating voltage is increased to a sufficient extent, the kinetic energy of the electrons becomes large enough to *excite* the mercury atoms in the tube. The electrons (c) thereby lose most of their kinetic energy and are no longer able to reach the detector electrode because they can't overcome the retarding potential V_d , and thus the voltage output drops significantly.

When the accelerating voltage is further increased, the collision zone moves progressively closer to the accelerating grid and the electrons which are initially braked by successful collisions are reaccelerated until their kinetic energy becomes large enough so that they collide with the mercury atoms once again and reexcite them (d). This energy transfer occurs periodically as the accelerating voltage increases.

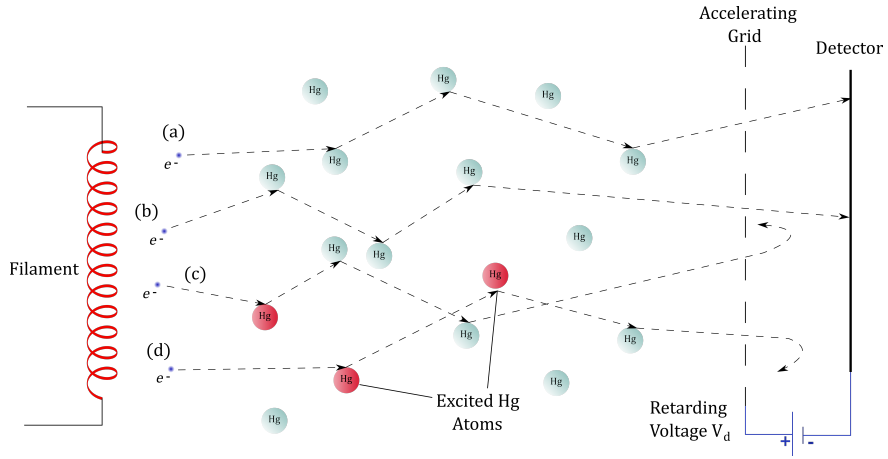


Figure 3: Types of electron-Hg collisions: (a), (b) Electrons don't possess enough kinetic energy to excite Hg atoms. (c) Electrons now experience a higher V_{acc} and excite Hg atoms, unable to reach the detector. (d) Electrons regain kinetic energy after V_{acc} is further increased and make multiple successful collisions, unable to reach the detector.

Experimental Procedure

We connect the control unit to the heating chamber and the Logger Pro as shown in Figure 4. The Logger Pro records the accelerating voltage in Channel 1 and the potential of the electrons as they reach the detector V_o in Channel 2. Notice on the upper right corner of the control unit that the recorded accelerating voltage in Channel 1 will be automatically divided by 10, thus we must multiply by this factor when plotting the data.

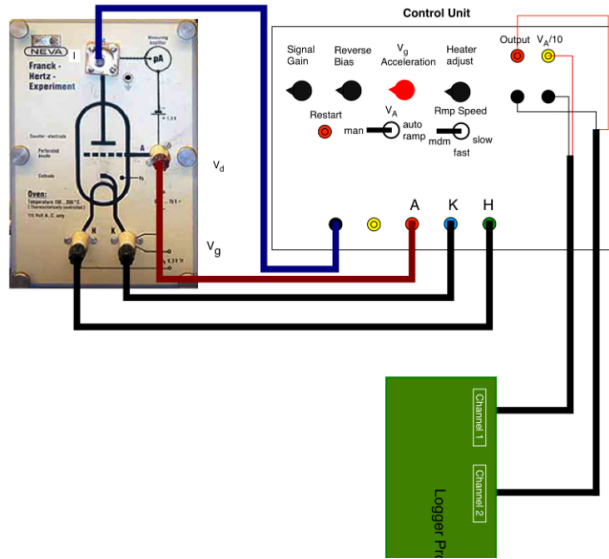


Figure 4: Experimental equipment complete diagram.

We turn on the heating chamber and set it to a temperature of 340°F for about 15 minutes to let the liquid mercury evaporate and enter dynamic equilibrium with its gas phase. The Hg gas exerts pressure on the walls of the Franck-Hertz tube equal to its vapor pressure at 340°F since no other

gases are present. We then supply the filament with a voltage of roughly 5.0 V using the Heater Adjust. A retarding voltage of 1.5 V will be set by rotating the Reverse Bias 45° counterclockwise. To begin taking data, we flip the V_A switch to Auto Ramp and press the Restart button. We collect data for about 15 seconds until the voltage output V_o becomes erratic. We repeat these steps at temperatures 400°F, 450°F, and 500°F.

3 Analysis

3.1 Mean and Uncertainty

Error in Quadratic Fit, Covariance

Around each peak, we fit a second order polynomial to estimate the accelerating voltage V_{acc} at which the electrons lose all their kinetic energy. That is, using a set of parameters a, b , and c to fit a parabola $y = ax^2 + bx + c$ through a set of data points, the maximum occurs at

$$\frac{dy}{dx} = 2ax + b = 0 \implies x_{\max} = -\frac{b}{2a} = V_{acc,\max}. \quad (1)$$

Now, x_{\max} is a function of the parameters a and b . Assuming that we can associate each output voltage V_{oi} with a count N_i , then there is a pair of measurements for each parameter, (a_i, b_i) . For the $N = \sum N_i$ measurements we can compute the means of the parameters, \bar{a} and \bar{b} , and so we can calculate the mean of x_{\max} , \bar{x}_{\max} . Assuming that the errors in a and b are small, we can expand Equation 1 as

$$x_{\max,i} \approx \bar{x}_{\max} + (a_i - \bar{a}) \frac{\partial x_{\max}}{\partial a} + (b_i - \bar{b}) \frac{\partial x_{\max}}{\partial b} \quad (2)$$

where $\bar{x}_{\max} = x_{\max}(\bar{a}, \bar{b})$. Therefore, the variance of x_{\max} is

$$\sigma_{x_{\max}}^2 = \frac{1}{N-1} \sum_{i=1}^N (x_{\max,i} - \bar{x}_{\max})^2. \quad (3)$$

Using Equation 2, Equation 3 becomes

$$\sigma_{x_{\max}}^2 = \frac{1}{N-1} \sum_{i=1}^N \left[(a_i - \bar{a}) \frac{\partial x_{\max}}{\partial a} + (b_i - \bar{b}) \frac{\partial x_{\max}}{\partial b} \right]^2 \quad (4)$$

Using the definition of variance on the parameters a and b we simplify the last equation to

$$\sigma_{x_{\max}}^2 = \left(\frac{\partial x_{\max}}{\partial a} \right)^2 \sigma_a^2 + \left(\frac{\partial x_{\max}}{\partial b} \right)^2 \sigma_b^2 + 2 \frac{\partial x_{\max}}{\partial a} \frac{\partial x_{\max}}{\partial b} \sigma_{ab} \quad (5)$$

Computing each partial derivative gives

$$\sigma_{x_{\max}}^2 = \frac{1}{4a^4} (b^2 \sigma_a^2 + a^2 \sigma_b^2 - 2ab \sigma_{ab}) \quad (6)$$

where we define the **covariance** σ_{ab} as

$$\sigma_{ab} = \frac{1}{N-1} \sum_{i=1}^N (a_i - \bar{a})(b_i - \bar{b}). \quad (7)$$

We can use Equation 7 for the error propagation of correlated variables. The **covariance matrix** is an $m \times m$ matrix whose entries are the covariances σ_{ij} , $i, j \in [x_1, x_2, \dots, x_m]$ of any set of m correlated variables.

Error of a Multivariable Function

If a multivariable expression F is a function of the independent variables x_1, x_2, \dots, x_n and if each variable has error $\sigma_{x_1}, \sigma_{x_2}, \dots, \sigma_{x_n}$, then the total error in F , σ_F , is

$$\sigma_F = \sqrt{\sum_{i=1}^n \left(\frac{\partial F}{\partial x_i} \sigma_{x_i} \right)^2} \quad (8)$$

Weighted Average and Error

For any discrete variable X estimated by subsequent measurements X_i , we can estimate its average \bar{X} and error $\sigma_{\bar{X}}$ by

$$\bar{X} = \frac{\sum X_i / \sigma_{X_i}^2}{\sum 1 / \sigma_{X_i}^2} \quad (9)$$

$$\sigma_{\bar{X}} = \sqrt{\frac{1}{\sum 1 / \sigma_{X_i}^2}}. \quad (10)$$

3.2 Results

In the following graphs we plot voltage output V_o as a function of the accelerating potential V_{acc} for temperatures 300°F, 400°F, 450°F, and 500°F. Around each peak, we fit a quadratic polynomial to estimate the accelerating voltages at which the electrons lost their kinetic energy due to collisions resulting excitation of mercury atoms. The energy difference ΔE between the ground and excited states of Hg, denoted as 1S_0 and 3P_1 respectively, is then equivalent to the energy difference between two successive peaks. That is,

$$\Delta E = e(V_{acc,n+1} - V_{acc,n}) \quad (11)$$

where e is the charge of the electron. Note that we did not add a subscript to the energy difference ΔE since we expect this quantity to be roughly constant due to the even spacing between successive peaks.

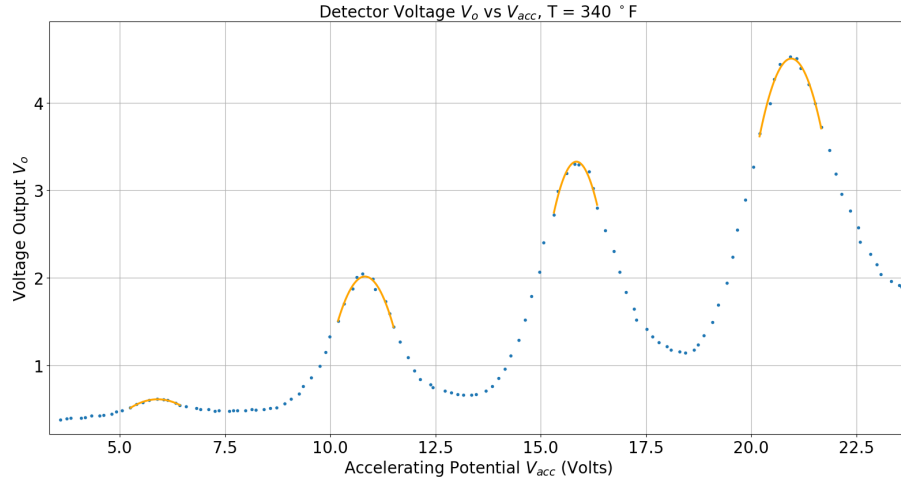


Figure 5: Data plot of V_o vs V_{acc} for experiment at 340°F

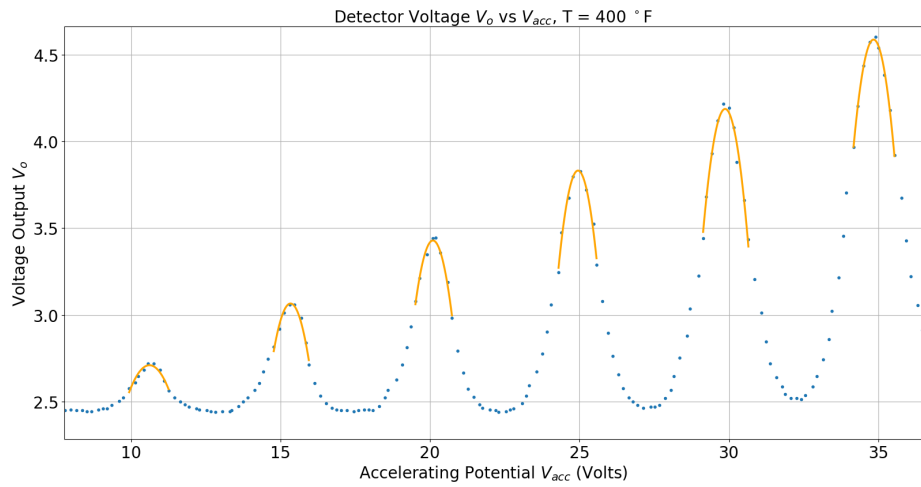


Figure 6: Data plot of V_o vs V_{acc} for experiment at 400°F

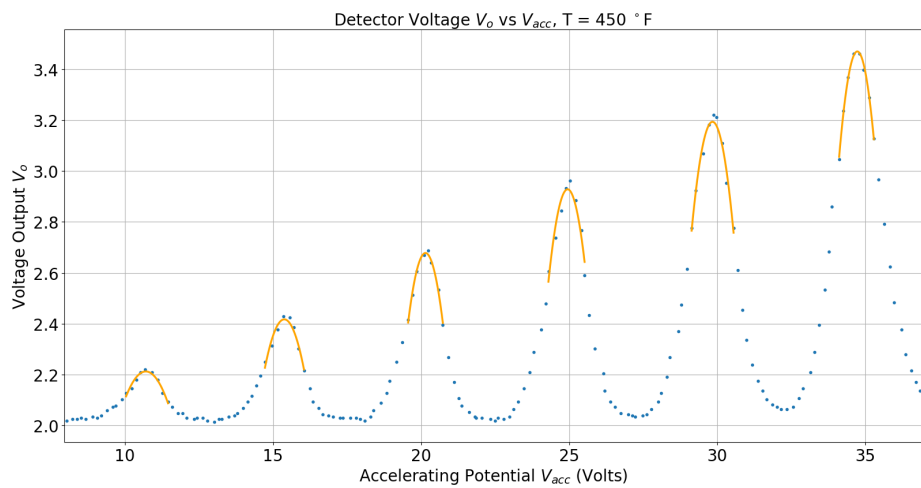


Figure 7: Data plot of V_o vs V_{acc} for experiment at 450°F

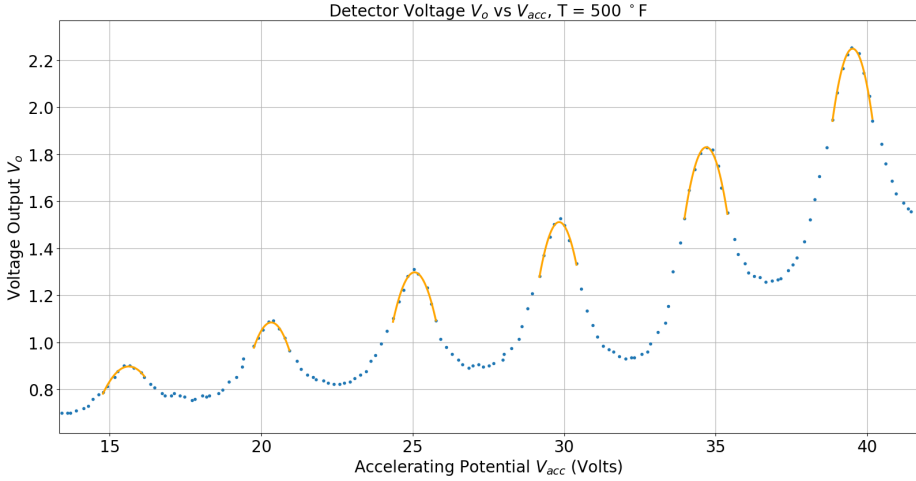


Figure 8: Data plot of V_o vs V_{acc} for experiment at 500°F

Each quadratic fit has the form

$$V_o = aV_{acc}^2 + bV_{acc} + c$$

where a , b and c are the parameters of the regression. Thus we can use Equations 1 and 6 to determine the centers of the peaks and their uncertainty from the covariance matrices calculated along with the fits. We compute such values in the following tables.

$T = 340^\circ\text{F}$		$T = 400^\circ\text{F}$	
$V_{acc,peak}$ (Volts)	$\sigma_{V_{acc}}$ (Volts)	$V_{acc,peak}$ (Volts)	$\sigma_{V_{acc}}$ (Volts)
5.898	1.0009	10.618	1.0035
10.821	1.0068	15.335	1.0062
15.845	1.0115	20.097	1.0058
20.948	1.0090	24.949	1.0079
		29.869	1.0082
		34.833	1.0032
$T = 400^\circ\text{F}$		$T = 500^\circ\text{F}$	
$V_{acc,peak}$ (Volts)	$\sigma_{V_{acc}}$	$V_{acc,peak}$ (Volts)	$\sigma_{V_{acc}}$ (Volts)
10.702	1.0024	15.628	1.0017
15.379	1.0051	20.327	1.0016
20.146	1.0030	25.060	1.0022
24.945	1.0111	29.830	1.0029
29.838	1.0063	34.688	1.0027
34.727	1.0029	39.517	1.0022

Table 1: Accelerating voltage peaks for each temperature setting.

To reiterate, we use Equation 11 to determine the energy difference between successive peaks, correlating to the energy of excitation of Hg atoms. The uncertainties are obtained through Equation 8 as

$$\sigma_{\Delta E} = e \sqrt{\sigma_{V_{acc,n+1}}^2 + \sigma_{V_{acc,n}}^2} \quad (12)$$

$T = 340^{\circ}\text{F}$		$T = 400^{\circ}\text{F}$	
ΔE (eV)	$\sigma_{\Delta E}$ (eV)	ΔE (eV)	$\sigma_{\Delta E}$ (eV)
4.9230	1.4197	4.7172	2.0127
5.0244	1.4272	4.7623	2.0110
5.1026	1.4287	4.8517	2.0253
		4.9196	2.0237
		4.9646	2.0121
$T = 450^{\circ}\text{F}$		$T = 500^{\circ}\text{F}$	
ΔE (eV)	$\sigma_{\Delta E}$ (eV)	ΔE (eV)	$\sigma_{\Delta E}$ (eV)
4.6770	2.0160	4.6991	2.0049
4.7674	2.0179	4.7329	2.0061
4.7992	2.0217	4.7708	2.0081
4.8928	2.0243	4.8574	2.0084
4.8894	2.0145	4.8292	2.0071

Table 2: Energy difference between consecutive peaks.

Next we tabulate the averages for ΔE and respective uncertainties at each temperature (Table 3) and plot them (Figure 9).

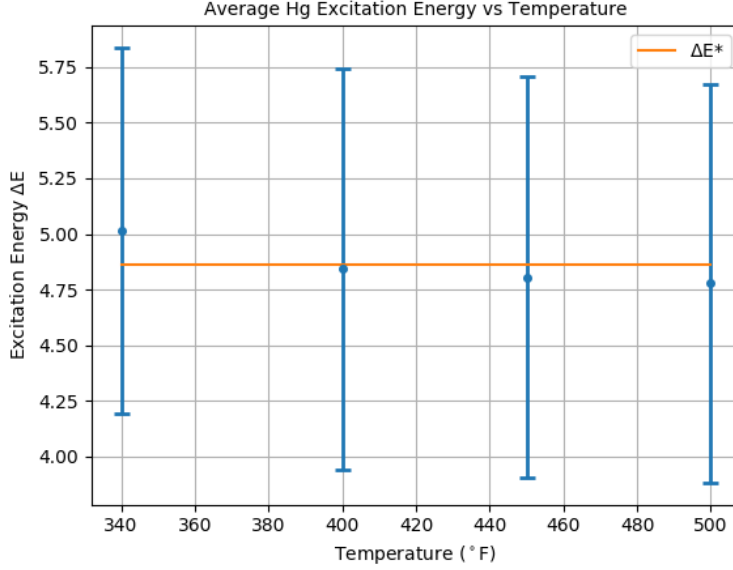


Figure 9: Average energy as a function of temperature. ΔE^* indicates the published value of the excitation energy of mercury² 4.86 eV.

Temperature (°F)	$\overline{\Delta E}$ (eV)	$\sigma_{\overline{\Delta E}}$
340	5.0162	0.8228
400	4.8430	0.9028
450	4.8049	0.9019
500	4.7778	0.8975

Table 3: Average excitation energy.

Taking the weighted averages of $\overline{\Delta E}$ in Table 3 gives us a final result for the $^1S_0 \rightarrow ^3P_1$ excitation potential of Hg vapor

$$\overline{\overline{\Delta E}} = (4.87 \pm 0.44) \text{ eV}$$

4 Conclusion

The excitation potential of mercury was measured to be (4.87 ± 0.44) eV, agreeing with the published value of 4.86 eV, 0.02 standard deviations off. As evidenced through Figure 9, altering the temperature did not affect our results significantly, although the most noticeable deviations originate at the lowest and highest temperatures. The former may be due to the fact that at a lower temperature, the intermolecular attractive forces between the gas particles and electrons play a more significant role. The gas molecules tend to interact a bit longer since they possess less average kinetic energy. This virtually reduces the probability of electron-Hg collisions and therefore electrons arrive to the detector with more kinetic energy, resulting in a higher output voltage. We can see in Figure 5 (experiment at 340°F) that by the 3rd peak, the voltage output is almost 4.5 V, whereas the only other graph that reaches a 4.5 V voltage output is Figure 6 ($T=400^\circ\text{F}$) but around its 6th peak, taking twice as long as the first set. Note that such pattern repeats as the temperature increases. The latter deviation may be explained in terms of vapor pressure and mean free path. Assuming that Hg gas particles possess a Maxwell distribution, it can be shown that the mean free path of an electron is roughly³

$$\ell = \frac{k_B T}{\sqrt{2\pi} d^2 p}$$

where k_B is the Boltzmann constant, d is the radius of a mercury atom, and p is the vapor pressure. Let us compare the mean free paths at $T = 300^\circ\text{F}$ (444.3 K) and $T = 500^\circ\text{F}$ (533.2 K). At 444.3 K and 533.2 K the vapor pressures of mercury are approximately 0.47 kPa and 7.0 kPa, respectively⁴. The radius of an Hg atom is 155 pm⁵.

$$\ell_{444 \text{ K}} = 3.06 \times 10^{-5} \text{ m} \quad \ell_{533 \text{ K}} = 2.46 \times 10^{-6} \text{ m}$$

The vapor pressure of mercury increases by about a factor of 15 at 533.2 K and so the mean free path is about 10 times shorter than at 444.3 K. This indicates that collisions will happen much more frequently at higher temperatures and therefore electrons will tend to lose more kinetic energy before reaching the detector, which is evidenced by the fact that Figure 8 possesses the lowest voltage outputs of the experiment. In summary, we were able to demonstrate the discreteness of the energy levels in mercury and the nature of the excitations involved in electron-Hg collisions accompanied with very accurate results.

5 References

- [1] Serway, Raymond A., et al. Modern Physics. Thomson Brooks/Cole, 2004.
- [2] <https://www.nist.gov/pml/atomic-spectra-database>
- [3] <http://hyperphysics.phy-astr.gsu.edu/hbase/Kinetic/menfre.html>
- [4] <https://www.govinfo.gov/content/pkg/GOVPUB-C13-66a1ade54071892930184393b1802e69/pdf/GOVPUB-C13-66a1ade54071892930184393b1802e69.pdf>
- [5] A. Bondi The Journal of Physical Chemistry 1964 68 (3), 441-451 DOI: 10.1021/j100785a001